Runge-Kutta Stellar Modelling and Support Vector Machine Zone Classification

Tristan Tipton[1]

[1]*Department of Physics and Astronomy, Texas A&M University, College Station, TX 77845*

(Dated: May 3, 2019)

Stellar Atmosphere theory has been known for some time. In this paper the author simulates this theory specifically for Homogenous Zero-Age Main Sequence Stars (ZAMS) using a Runge-Kutta Algorithm and then takes the data provided from the theoretical calculations and attempts to classify the different zones of a star using Radial Basis Function (RBF) Support Vectors and Linear Support Vectors so that the trained Support Vector Machine (SVM) may be used on any given stellar data to classify that star's stellar zones.

I. INTRODUCTION

Stellar modelling is a subject of interest to many astronomers, astrophysicists, and plasma physicists alike because the ability to simulate what is going on in a star can tell one a great number of things about the physics of the star since it is not possible otherwise to do so. In this paper the author will attempt to do the same thing for ZAMS stars by going over the theory first, the algorithm used second, the classification model third, the data fourth, and then finally the analysis and conclusion.

II. STELLAR ATMOSPHERE THEORY

Here the author describes in short detail the inner workings of a star and the necessary equations to perform the evaluation of the Runge-Kutta Algorithm.

A. Basic Assumptions and Definitions

Stars are ever-changing objects with many varying parameters. In order to make this simulation run more smoothly the author chooses to assume the the simulated stars are homogeneous and static. This is a key feature in ZAMS stars.

Furthermore, the author assumes that the pressure, mass, density, luminosity and temperature are functions of the radius of the star (P, M, ρ, L and T respectively). Therefore at $r = R$, the radii of the star, each value takes on either its total or surface value which will be indicated with a subscript "R". The author will also assume that the furthermost zone of the star is completely radiative or convective.

The final definition needed is the one that defines when a star is convective. This transition from radiative to convective occurs when the temperature gradient becomes superadiabatic. In this case this happens when

$$\frac{d(lnP)}{d(lnT)} < 2.5 \tag{1}$$

Physically this is because the opacity of the star begins to inhibit the radiative transport of energy to the outer shells [1].

B. Equations

Since these stars are static there is no time component in any of the following equations [1].

$$\frac{dP}{dr} = -G\frac{M\rho}{r^2} \tag{2}$$

Here G is the universal gravitational constant.

$$\frac{dM}{dr} = 4\pi r^2 \rho \tag{3}$$

$$\frac{dL}{dr} = 4\pi r^2 \rho \epsilon \tag{4}$$

ϵ is the total energy released by all the nuclear reactions within the star plus the energy released from gravitational contraction. The gravitational contraction of the star is ignored, however, because the star is assumed to be static.

$$\frac{dT}{dr} = -\frac{3}{4ac}\frac{\bar{\kappa}\rho}{T^3}\frac{L}{4\pi r^2} \tag{5}$$

$\bar{\kappa}$ is the Total Rosseland mean opacity, a is the radiation constant and c is the usual speed of light in a vacuum.

C. Boundary Conditions

In order for this program to work one needs to operate off of certain boundary conditions. The luminosity and mass must go to zero as $r \to 0$. Furthermore, the temperature, pressure and the density must also go to zero as $r \to R$ [1].

These boundary conditions simplify the limits of integration within the code and are easy to understand. In practicality, these conditions do not always go to zero in most circumstances [1].

D. Derivation of Useful Equations

Now that the basic assumptions, definitions and equations are stated one may derive useful relations for the program as stated in Carroll & Ostlie [1]. Consider a radiative zone first, take equation (2) and (5) and divide them. This results in

$$\frac{dP}{dT} = \frac{16\pi ac}{3}\frac{GM_R}{L_R}\frac{T^3}{\bar{\kappa}} \tag{6}$$

At the outer layer of the hypothetical star the likelihood of many free electrons or ions is small so one may assume their contribution to $\bar{\kappa}$ is zero. This results in a $\bar{\kappa}$ that is equivalent to the sum of bound-free and free-free Kramers opacity laws. The author will define the the sum of both to be κ_f. Rewriting (6) in terms of their values and utilizing the ideal gas law gives

$$\frac{dP}{dT} = \frac{16\pi}{3}\frac{GM_R}{L_R}\frac{ack_B}{\kappa_f \mu m_H}\frac{T^{7.5}}{P} \tag{7}$$

where k_B is Boltzmann's constant, m_H is the mass of the hydrogen atom and μ is the mean molecular weight.

Assuming everything else is held constant one can now treat $P(r)$ as $P(T)$. To find this equation one must integrate (7) with respect to the temperature of the star. Doing so yields

$$P = \left(\frac{1}{4.25}\frac{16\pi}{3}\frac{GM_R}{L_R}\frac{ack_B}{\kappa_f \mu m_H}\right)^{1/2} T^{4.25} \tag{8}$$

Now using equation (5), Kramers and ideal gas laws one can get T(r) as follows

$$T = GM_R\left(\frac{\mu m_H}{4.25k_B}\right)\left(\frac{1}{r} - \frac{1}{R}\right) \tag{9}$$

Equation (9) will be used to obtain the value for the temperature in the star at any given r and then this value will be returned to equation (8) to obtain the pressure value at that point. Now that both of these are available one can obtain the density, opacity, and the total energy parameter by using thermodynamic equations of state.

Now consider a convective zone. If one rewrites equation (5) as

$$\frac{dT}{dr} = -\left(1 - \frac{1}{\gamma}\right)\frac{\mu m_H}{k_B}\frac{GM}{r^2} \tag{10}$$

and integrates the equation with the assumption that the adiabatic relation between specific heats γ is constant then we obtain

$$T = GM_R\left(\frac{\gamma - 1}{\gamma}\right)\frac{\mu m_H}{k_B}\left(\frac{1}{r} - \frac{1}{R}\right) \tag{11}$$

In a similar manner to finding the quantities related to equation (9), one may obtain the pressure in this case by utilizing an equation of state dependent on adiabatic pressure.

To obtain values for the star in its interior one must integrate. Changing equation (2) into

$$\frac{dP}{dr} = -\frac{4\pi}{3}G\rho_0^2 r \tag{12}$$

where ρ_0^2 is the squared mean density of the previously calculated zone in the star. Multiplying through both sides with dr and integrating both results in an equation for the central pressure of the star.

$$P_0 = P + \frac{2\pi}{3}G\rho_0^2 r^2 \tag{13}$$

There are other values that are obtained from this as well and can be found on page A-25 of Carroll & Ostlie.

III. RUNGE-KUTTA ALGORITHM

The integration performed in this program utilizes a Fourth Order Runge-Kutta Algorithm. It evaluates some of the previously mentioned equations at different intermediate points [1]. The general form of the Runge-Kutta Algorithm is shown here

$$y_{n+1} = y_n + \frac{k_1}{6} + \frac{k_2}{3} + \frac{k_3}{3} + \frac{k_4}{6} + O(h^5) \tag{14}$$

where h is the step to be taken and k_i is a function of the step multiplied by the evaluation of dy_n/dx_n at some step smaller than h [6].

The code written by Carroll & Ostlie and edited by Dr. Schiminovich and the author can be found at this url: `https://github.com/senortipton/ASTRC3101/blob/master/StatStar.py`. The code previous to the author's edit can be found at: `https://github.com/rasmi/ASTRC3101/blob/master/HW2/statstar.py` [1][7].

IV. SUPPORT VECTOR MACHINE

The code used for this section will be included at the end of the paper and utilizes a random training/test data split of 20%/80% [2][3][4][5][8].

Using this method one can attempt to classify the zones of a star based on many different parameters. By having the model train on the train data set one can then attempt to see if the model predicts the correct values for the testing set. In general, if the predictions more or less match the testing data set then the model is likely a good one. Knowing what the stellar theory says for classification the author excluded certain parameters that did not peak in higher radii.

A. Radial Basis Function

The choice to use RBF SVM's to perform the machine learning on this data was made with the realization that the theory suggests that the linear SVM would not be able to classify accurately with the potential for the radiative zone to have temperature gradient values that are similar to the convective zone. The goal here was to obtain values for different stars and see if the machine could predict the classification of the star without knowing anything about the physical laws that describe it as such.

RBF SVM's are defined mathematically as follows [9]:

$$\mathbf{K}(\vec{x}, \vec{x}') = e^{-\frac{||\vec{x}-\vec{x}'||^2}{2\sigma^2}} \tag{15}$$

$\vec{x}$ and $\vec{x}'$ are vectors of independent variable values. σ defines a radius for which to classify different resultant values of the two vectors. In a 2-D case the resultant space is 3-D where $\vec{x}$ and $\vec{x}'$ correspond to x and y and the resultant value of both becomes z. If one maps the values back to 2-D space the classification regions are defined by σ.

B. Linear SVM

The linear SVM is similar to the RBF in that it solves the problem in a higher dimension and then maps the solution to the original dimension with the exception that the classification separator will not be a curved and enclosed region(s), instead it is separated exactly by a linear equation. The SVM will find the best linear equation to separate most of the unrelated data to each classification and then return it.

The real power that this classification model has in this circumstance is that it has the potential to classify the entire region depicted for stellar zones as shown in Carroll & Ostlie [1].

V. DATA

The author presents the various values compared to the radius of three different trial stars (listed in TABLE I.) in the subsection "Runge-Kutta Data" as well as presenting the case of pressure dependence on temperature. Data pertaining to the SVM is listed in "SVM Data".

TABLE I. Input Parameters for "StatStar.py"

Parameter	Star 1	Star 2	Star 3
Mass $\frac{M}{M_\odot}$	1	0.75	1
T_{Eff} (K)	5.5002E03	3.8391E03	5772
L $\frac{L}{L_\odot}$	8.6701E-01	1.877E-01	1
X (% Hydrogen)	70	70	74
Z (% Metals)	0.8	0.8	2

A. Runge-Kutta Data

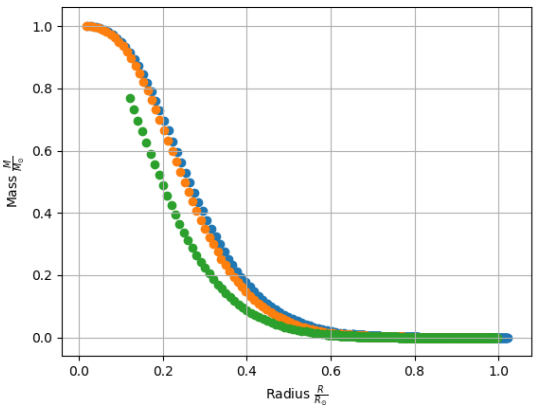

FIG. 1. Star Radius and Mass. Data is oriented such that the graph reflects where the majority of mass is found. Colors "blue", "orange" and "green" correspond to "Star 1", "Star 2" and "Star 3" in that order.

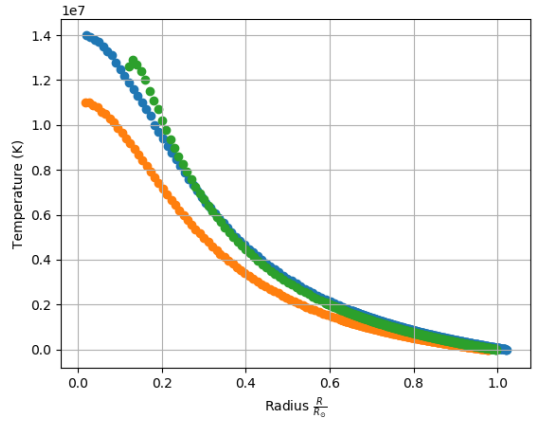

FIG. 2. Star Radius and Temperature. Colors "blue", "orange" and "green" correspond to "Star 1", "Star 2" and "Star 3" in that order.

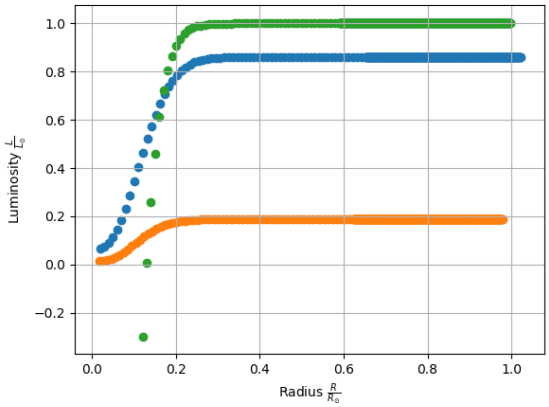

FIG. 3. Star Radius and Internal Luminosity. Colors “blue”, “orange” and “green” correspond to “Star 1”, “Star 2” and “Star 3” in that order.

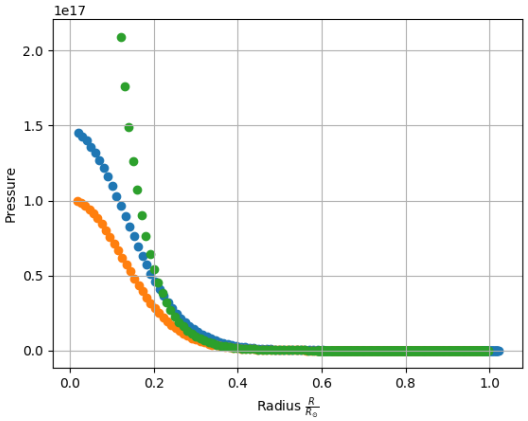

FIG. 5. Star Radius and Pressure. Colors “blue”, “orange” and “green” correspond to “Star 1”, “Star 2” and “Star 3” in that order.

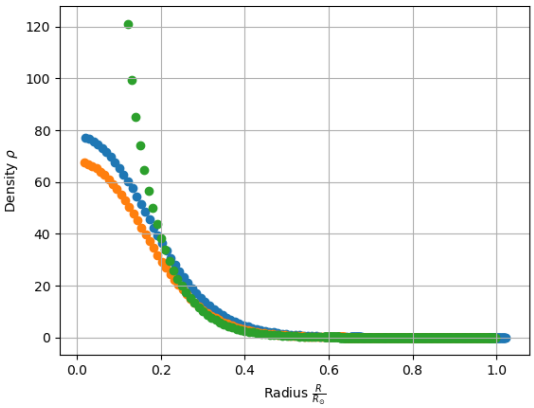

FIG. 4. Star Radius and Density. Colors “blue”, “orange” and “green” correspond to “Star 1”, “Star 2” and “Star 3” in that order.

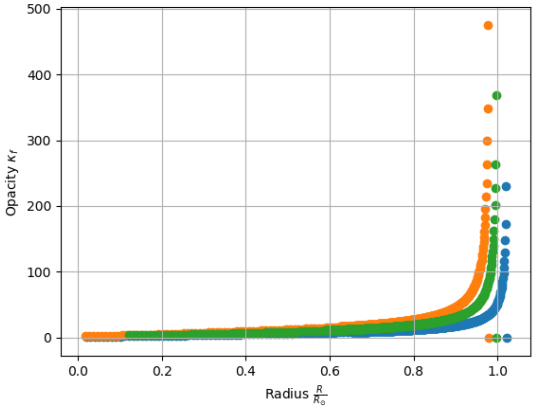

FIG. 6. Star Radius and Opacity. Colors “blue”, “orange” and “green” correspond to “Star 1”, “Star 2” and “Star 3” in that order.

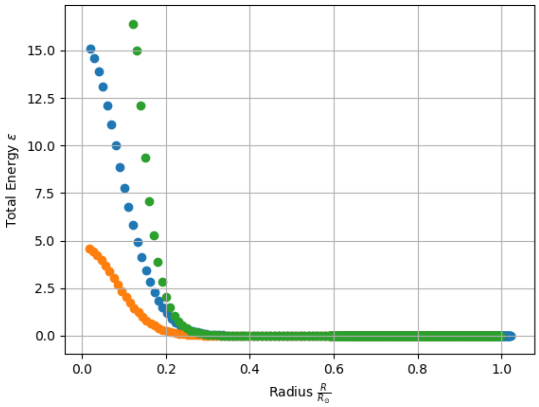

FIG. 7. Star Radius and Total Energy. Colors "blue", "orange" and "green" correspond to "Star 1", "Star 2" and "Star 3" in that order.

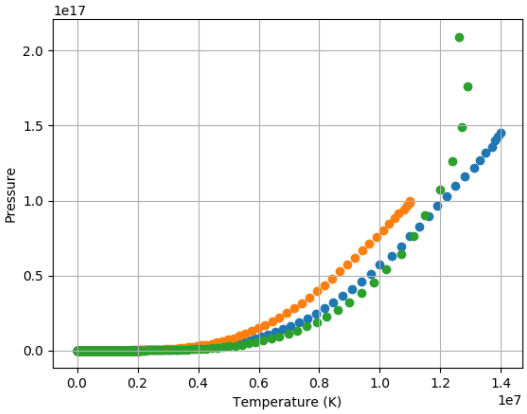

FIG. 9. Star Temperature and Pressure. Colors "blue", "orange" and "green" correspond to "Star 1", "Star 2" and "Star 3" in that order.

B. SVM Data

Data pertaining to correct and incorrect classification predictions are listed in confusion matrix tables and correspond to the training and test data of "Star 1" herein. Confusion matrices show the number of false positives and negatives versus true positives and negatives for the classification prediction of multiple independent variables. Figures of classification predictions are shown after each corresponding confusion matrix that accepts two independent variables.

TABLE II. RBF Confusion Matrix for Radius and Temperature Gradient

	Pred. Convective	Pred. Radiative
Actual Convective	0	4
Actual Radiative	0	124

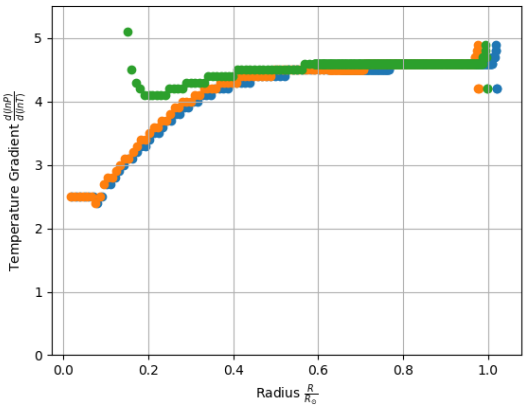

FIG. 8. Star Radius and Temperature Gradient. Colors "blue", "orange" and "green" correspond to "Star 1", "Star 2" and "Star 3" in that order.

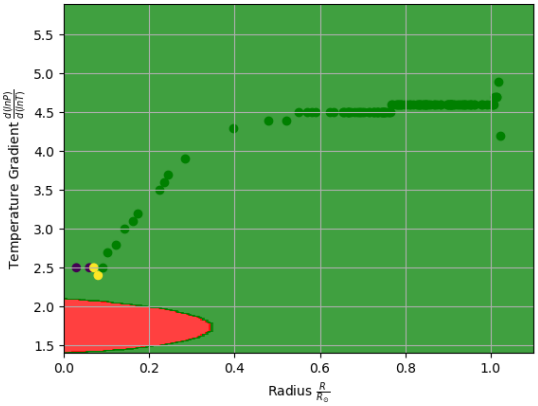

FIG. 10. RBF Classification Using Radius and Temperature. "Red" is "Convective" and "Green" is "Radiative".

TABLE III. Linear Confusion Matrix for Radius and Temperature Gradient

	Pred. Convective	Pred. Radiative
Actual Convective	0	4
Actual Radiative	0	124

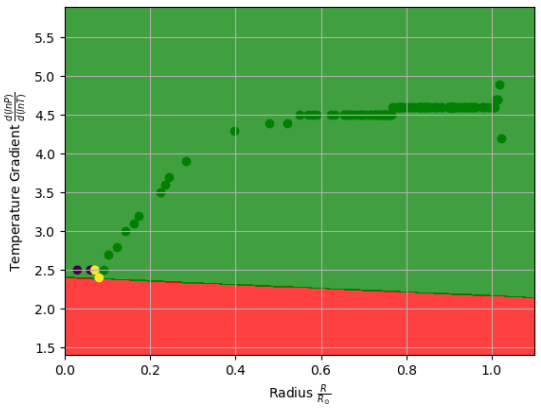

FIG. 11. Linear Classification Using Radius and Temperature. "Red" is "Convective" and "Green" is "Radiative".

TABLE IV. RBF Confusion Matrix for Radius and Opacity

	Pred. Convective	Pred. Radiative
Actual Convective	0	4
Actual Radiative	0	124

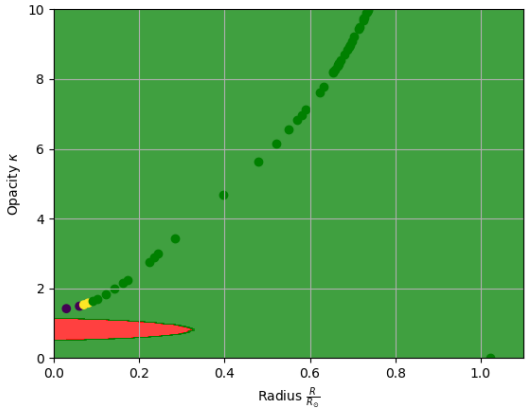

FIG. 12. RBF Classification Using Radius and Opacity. "Red" is "Convective" and "Green" is "Radiative".

TABLE V. Linear Confusion Matrix for Radius and Opacity

	Pred. Convective	Pred. Radiative
Actual Convective	3	1
Actual Radiative	1	123

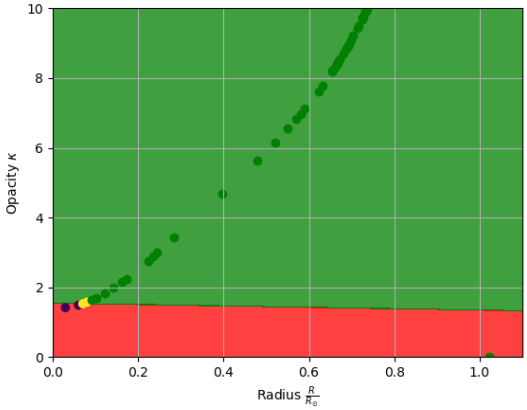

FIG. 13. Linear Classification Using Radius and Opacity. "Red" is "Convective" and "Green" is "Radiative".

TABLE VI. RBF Confusion Matrix for Temperature Gradient

	Pred. Convective	Pred. Radiative
Actual Convective	4	0
Actual Radiative	1	123

TABLE VII. RBF Confusion Matrix for Opacity

	Pred. Convective	Pred. Radiative
Actual Convective	3	2
Actual Radiative	0	124

TABLE VIII. RBF Confusion Matrix for Opacity and Temperature Gradient

	Pred. Convective	Pred. Radiative
Actual Convective	4	0
Actual Radiative	0	124

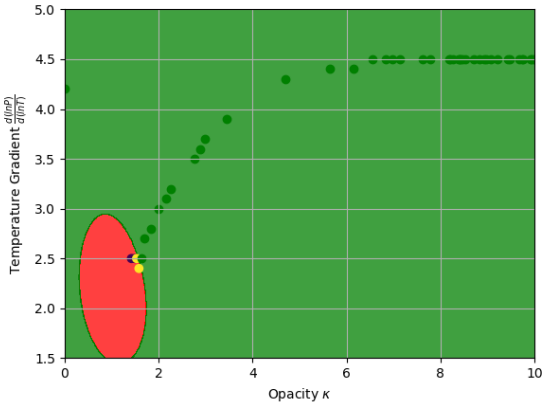

FIG. 14. RBF Classification Using Opacity and Temperature Gradient. "Red" is "Convective" and "Green" is "Radiative".

TABLE IX. Linear Confusion Matrix for Opacity and Temperature Gradient

	Pred. Convective	Pred. Radiative
Actual Convective	4	0
Actual Radiative	3	121

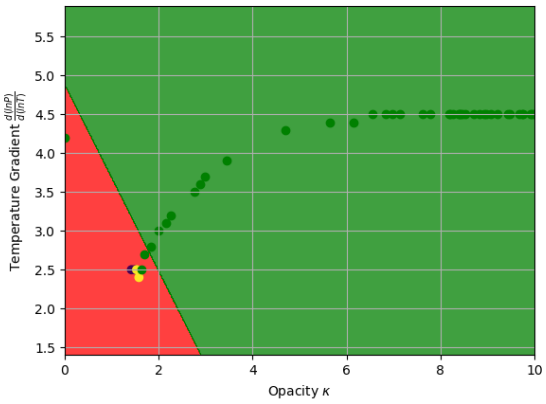

FIG. 15. Linear Classification Using Opacity and Temperature Gradient. "Red" is "Convective" and "Green" is "Radiative".

VI. ANALYSIS

In this section the author discusses the results from both the Runge-Kutta Algorithm evaluation of the input parameters in TABLE I and then moves onto SVM.

A. Runge-Kutta Analysis

For this data the author used inputs "Star 1" and "Star 2" as acceptable ZAMS stars. The author then used the sun to compare to to test the effectiveness of the model. The difference between the model's affect on the test stars' and sun's values becomes immediately apparent in FIG.1. One can see that while the test stars have a significant portion of their mass near the center, the sun falls short by about $0.2M_{\odot}$. This shortcoming is already evidence that the model is both simple and inaccurate to what society knows today about actual stars.

In FIG. 2 the temperature of the sun behaves like the other ZAMS stars at larger radii, but near the center it once again fails to evaluate all the way to the center and even shows that it might begin to decrease in temperature near the core. Outside of this region the stars behave as expected according the boundary conditions set forth earlier.

FIG. 3 is the main issue for testing the model on the sun. When evaluating the internal luminosity of the sun the model evaluates to a negative luminosity. This is not acceptable because a negative luminosity means that instead of the sun radiating away energy to the outside it actually absorbs the energy instead. Of course absolute magnitude can be negative, but since the luminosity in this case is calculated as a ratio of the target star's luminosity compared to the sun's it cannot be less than or equal to zero. Outside of the smaller radius region the sun does agree with the ZAMS stars as all of them quickly reach their peak luminosity and do not increase thereafter.

The density and pressure of the stars as shown in FIG. 4 & 5 behave like a sigmoid, rapidly decreasing in value as radius increases. In fact, the density decreases so fast that it almost reaches zero at about halfway through the radius of the stars. The sun mostly follows this trend with the exception that the density appears to be exponentially increasing as radius decreases.

FIG. 6 is the first case in which a star of lesser mass has a higher value than the other stars. In this case it seems that the stars have more or less the same opacity in the interior until they reach a certain radius, after which they begin to rapidly increase in opaqueness. Furthermore one can see that for the less massive star that not only does the increase in opaqueness happen at a lesser radius, it also continues to a much higher value indicating that less massive stars are much less likely to allow radiative transport of energy.

The total energy the star creates in this model (FIG. 7) completely ignores energy conversion from gravitational contraction to heat since these stars are static. That being said, the ability for nuclear reactions still occur as is typical with ZAMS stars. As expected, the stars with higher mass and greater T_{Eff} exude more energy production. Also, all of them quickly decay in energy production once the radius is no longer within the realm of the core of these stars.

The temperature gradient of these stars (FIG. 8) mostly behaves as expected [1]. The sun's temperature gradient rapidly increases closer towards the core when it should be actually decreasing. The other two stars behave fairly well in this case and all three behave exactly as expected for the region in half the radius. After this region all three stars fail to behave as expected and should actually decrease to a minimum of about 2.5 near the surface of each star. This shortcoming of the model means that the classification of zones later will be incorrect, not because the classification fails but rather because the convective zone must occur at a radius where the temperature gradient meets a second minimum.

The last figure, FIG. 9, is a representation of the previously solved equation (8). As expected of an ideal gas approximation, the temperature and gas increase together. The rate at which they increase appears to be exponential, especially in the case of the sun. Although there does appear to be an issue with this part of the model as well. The sun rapidly increases in pressure as temperature changes, but at one point it increases rapidly and then quickly decreases as well. This is atypical of any star and is another indication of a failure of the model.

B. SVM Analysis

Even though the data here is inaccurate due to the model not accurately calculating the temperature gradient, it does not invalidate the possibility of this method to classify the stellar atmospheric zones.

TABLE I-III and FIG. 10-11 look at the possibility of classifying the different stellar zones by choosing the independent variables as the radius and temperature. One can clearly see that both the RBF and linear model do not classify the "convective" zone at all (quotations because RBF red region fits the criterion for the temperature gradient, but does not meet the criterion for radius). The linear model does a good job of potentially picking up any convective zones at a greater radius but the potential for this is inhibited by the stellar model. Besides the figure, the failure to classify is immediately evident by the confusion matrix as no data that should be classified a convective zone is, in actuality, convective.

The next pairs of data (TABLE IV-V and FIG. 12-13) showcases the classification using radius and opacity. The RBF classification model fails for the same reason and does not manage to get anywhere closer to classifying them accurately. The combination of both failures while utilizing the radius means that the radius has three possible reasons for the failure to classify. The first reason is that the radius may have no bearing on the classification. One knows this reason to be false if the theory is true. The second reason is that the radius negatively impacts the classification and the third is that there isn't enough data on the relationship between radius and opacity or the temperature gradient. Reason two is unlikely for the same idea as why reason one fails. This means that in all likelihood reason three is the main culprit. This analysis is also evidenced by the shortcomings of the model in FIG. 8. The linear model does a great job of classification with a convective prediction accuracy of 75% and radiative prediction accuracy of 99.1%. This suggests that the radius, and by extension the linear model, does indeed play a part in the determination of stellar zones which is contrary to the RBF model of the same data. This evidence, despite the disagreement between the models, supports the known theory as well.

The last tables (TABLE VI-IX) and FIG. 14-15 demonstrate the RBF and linear classification models were indeed successful. The individual testing of the importance of classification by just using the temperature gradient or opacity by themselves showed that the RBF model predicted the zone with 100% accuracy for convective and 99.1% accuracy for radiative in the case of the temperature gradient and 60% accuracy for convective and 100% accuracy for radiative in the case of the opacity. These numbers are preliminary and do not indicate the actual accuracy of the model with a larger data set as it is likely these accuracies would be a bit lower. That being said, the RBF model clearly indicates that there is a correlation with stellar zones and the temperature gradient and/or the opacity which corroborates what one knows to be true in the theory. The last two confusion matrices combine both the temperature gradient and the opacity and shows the accuracy for the model trained on both. In this case one can see that the RBF model predicts 100% accuracy for both zones and the linear model predicts 100% for convective and 97.5% for radiative, but is still likely to be less accurate due to it being preliminary. Looking at the figures representing this data one can observe that while these models have correctly identified what region the temperature gradient is superadiabatic, they still fall short because they have classified a low opacity as relevant to the outcome of the zone type which is opposite what the theory says. The author knows this to be a fault of the stellar model as opposed to the SVM models for reasons mentioned earlier.

VII. CONCLUSION

The author was able to run a mostly successful stellar model of two different ZAMS stars and the sun. While the two ZAMS stars behaved as expected from the initial assumptions, definitions and boundary conditions, the sun failed to behave as expected in the model despite itself being on the main sequence. This indicates that while the stellar model is a good rough approximation for the modelling of stellar interiors, it cannot successfully handle actual star data.

The SVM models trained on the data obtained from the stellar model proved to be accurate and precise, but not effective. The classification model was able to determine that the temperature gradient and opacity of the

star were the important indicators for the classification of a stellar zone, but ultimately failed because it knows nothing about the physics of the problem (i.e. the model should have classified higher opacity). That being said, with more data that is able to fill out the entirety of a star's temperature gradient curve the model may be able to effectively classify the stellar zones within a star.

In the future the author would like to improve this model to be able to handle real world star data, specifically the temperature gradient, and then try to implement the SVM model on the data again.

ACKNOWLEDGMENTS

The author is grateful for GitHub and GitHub user "rasmi" for posting a Python 2 version of code (written by Prof. D. Schiminovich of Columbia University Department of Astronomy) for which the author could add to, work on and apply the machine learning model.

[1] B. W. CARROLL and D. A. OSTLIE. *An introduction to modern astrophysics*, pages 330–334, 354–355, A23–A25. Pearson-Addison-Wesley, San Francisco, second edition, 2007.

[2] J. D. HUNTER. Matplotlib: a 2d graphics environment. *Computing in Science & Engineering*, 9:90–95, 2007.

[3] W. MCKINNEY. Data structures for statistical computing in python, 2010.

[4] T. E. OLIPHANT. A guide to numpy, 2006.

[5] F. PEDREGOSA, G. VAROQUAUX, A. GRAMFORT, V. MICHEL, B. THIRION, O. GRISEL, M. BLONDEL, P. PRETTENHOFER, R. WEISS, V. DUBUORG, J. VANDERPLAS, A. PASSOS, D. COURNAPEAU, M. BRUCHER, M. PERROT, and E. DUCHENSAY. Scikit-learn: machine learning in python. *Journal of Machine Learning Research*, 12:2825–2830, 2011.

[6] W. H. PRESS, S. A. TEUKOLSKY, W. T. VETTERLING, and B. P. FLANNERY. *Numerical recipes in c*, pages 710–712. Cambridge University Press, second edition, 1992.

[7] D. SCHIMINOVICH. Modern stellar astrophysics. `https://github.com/rasmi/ASTRC3101`, Jan 2016. Accessed on 2019-4-30.

[8] S. VAN DER WALT, C. COLBERT, and G. VAROQUAUX. The numpy array: a structure for efficient numerical computation. *Computing in Science & Engineering*, 13:22–30, 2011.

[9] J. VERT, K. TSUDA, and B. SCHOLKOPF. A primer on kernel methods, 2004.